Diluted antiferromagnets in a magnetic field: A fractal-domain state with spin-glass behavior

U. Nowak* and K. D. Usadel
Theoretische Tieftemperaturphysik, Universität Duisburg, Lotharstrasse 1, 4100 Duisburg 1, Germany
(Received 30 May 1991)

The phase diagram of diluted Ising antiferromagnets in the limit of high external magnetic fields B and strong dilution is investigated by a Monte Carlo simulation. The two relevant lines in the B-T plane of the phase diagram, $B_{eq}(T)$ which marks the onset of hysteretic effects and $B_c(T)$ above which antiferromagnetic long-range order is no longer stable are determined. Between these two lines there is a broad range of high fields and low temperatures with the characteristics of a frozen domain state. The irreversibilities observed in this state and the scaling behavior of $B_{eq}(T)$ both give evidence for the occurrence of a spin-glass phase. A further investigation of the relevant scaling laws for the domains leads to the conclusion that the domain state consists of fractal domains becoming stable for high magnetic fields.

I. INTRODUCTION

There have been several studies on the behavior of random-field systems. Experiments are normally performed on diluted Ising-type antiferromagnets in a uniform external magnetic field (DAFF) which belong to the same universality class as the random-field Ising model (RFIM).[1] Surprisingly, the phase diagram of the DAFF in the limit of strong disorder and high fields is still not very well understood despite many efforts. Several possibilities have been discussed in the literature: (i) the existence of a transition from antiferromagnetic order to paramagnetic behavior which is of second order for all temperatures;[2] (ii) the existence of a tricritical point with a crossover to a first order transition for low temperatures;[3] (iii) the existence of a spin-glass phase for low temperatures and high fields;[4,5] and (iv) the existence of a stable domain state.[6]

The complexity of the problem is due to the formation of a domain state with extreme relaxation times, a characteristic feature of the DAFF. This domain state is thought to be metastable for lower fields. It is obtained by cooling the system in an external field from the paramagnetic high temperature phase. From neutron scattering experiments it was concluded that this field cooled state is frozen at low temperatures.[7] The mechanisms which are responsible for the corresponding hysteretic properties of the DAFF have been investigated experimentally,[7,8] theoretically,[9] and in computer simulations.[6,10] Apart from this a non-exponential decay of the remanent magnetization of the field cooled state after switching off the external field has been found experimentally[8] and further investigated theoretically,[11] and in computer simulations, respectively.[12]

In this paper we want to focus on the phase diagram of the DAFF and the physics of the domain state, especially its thermodynamic properties, scaling behavior, and fractality. The paper is organized as follows.

In the second section we will describe the methods to determine the relevant lines of the phase diagram, i.e., $B_{eq}(T)$ marking the onset of hysteretic effects and $B_c(T)$ above which antiferromagnetic long-range order is no longer stable.

In the third section we analyze and discuss the phase diagram. For high magnetic fields we find a scaling behavior for $B_{eq}(T)$ roughly in agreement with the de Almeida–Thouless (AT) line known from the conventional Ising spin glasses[13] which we consider to give evidence for a spin-glass-like behavior. This result is supported by recent experimental investigations of strongly diluted $FeZnF_2$ in high magnetic fields.[5]

In Sec. IV we endeavor for a deeper insight in the physics of the high field domain state. The domains turn out to be fractal with a scaling behavior deviating from the usual assumption of the Imry-Ma argument[14] which of course is only expected to be valid in the limit $B \to 0$.

II. DETERMINATION OF THE PHASE DIAGRAM

The Hamiltonian of the DAFF in units of the coupling constant J reads

$$H = \sum_{\langle i,j \rangle} \epsilon_i \epsilon_j \sigma_i \sigma_j - B \sum_i \epsilon_i \sigma_i, \tag{1}$$

where $\sigma_i = \pm 1$ and $\epsilon_i = 0, 1$. Only nearest neighbor interaction is considered. In our Monte Carlo simulation[15] we used helical boundary conditions and the heat-bath algorithm. The size of the system during the simulation of the phase diagram was $61 \times 61 \times 60$. For the investigation of the structural properties of the domain state we simulated systems with a size of up to $145 \times 145 \times 144$ spins in order to observe even larger domains. The di-

lution was 50%. The program was written in C and the simulation was done on an IBM RS6000 workstation.

In order to determine the phase diagram we computed the magnetization $M(T)$ and the internal energy $E(T)$ during field cooling (FC) from the completely disordered paramagnetic state and field heating (FH) from the long-range ordered antiferromagnetic state (for details see Ref. 10). Due to the freezing of the system during FC there occur irreversibilities the onset of which marks $B_{eq}(T)$. Figure 1 shows four of the computed $E(T)$ loops. The heating or cooling rate was 100 Monte Carlo steps (MCS) per point with a corresponding temperature interval of 0.01. For low B the energy of the system during FH is lower than during FC (upper curve). The opposite behavior is found for higher fields where the domain state reached upon FC carries less internal energy (the two lowest curves). In the crossover region the difference between the energies of FC and FH procedure is too small to determine $B_{eq}(T)$ (see the loop for $B = 1.2$ in Fig. 1). But in this region information can be gained from the corresponding magnetization loops.

Figure 2 shows $M(T)$ loops for the same fields as in Fig. 1. The magnetization during FC is always higher except in the limit of very high fields where there is practically no significant difference between the two magnetization curves. Therefore, in comparing $E(T)$ and $M(T)$ loops we have the possibility to determine $B_{eq}(T)$ for all possible values of B. The corresponding data $B_{eq}(T)$ obtained from extensive Monte Carlo simulations are summarized in the phase diagram Fig. 3 where we used triangles for the $M(T)$ data and crosses for the $E(T)$ data.

The second relevant line in the phase diagram is $B_c(T)$. In Fig. 1 the energy obtained through FH is smaller than the energy obtained through FC for low fields. Hence in this regime we can conclude, that a long-range ordered state is the stable ground state for $T \to 0$. This behavior

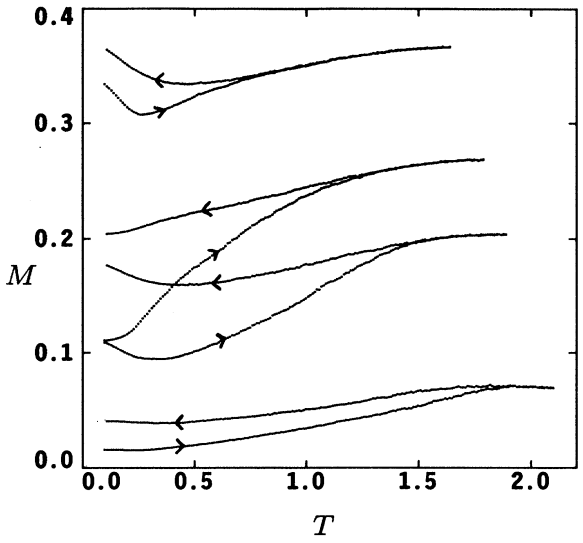

FIG. 2. Magnetization vs temperature as in Fig. 1

is reversed for higher fields where the energy obtained through FC is the smaller one. Hence we conclude that the domain state is the stable phase for higher fields. Therefore, in the low temperature regime we can estimate $B_c(T \to 0)$ as that field where practically no difference in the energy of the FC and FH loops for $T \to 0$ occurs. This point is marked in the phase diagram by a circle on the B axis.

In order to further estimate the critical line we have looked for the maximum of $\partial M/\partial T$ during FH which marks the critical temperature in the crossover regime from random exchange to random field behavior,[16] i.e., in the limit of small B. The corresponding data $T_c(B)$ are shown as filled circles in Fig. 3.

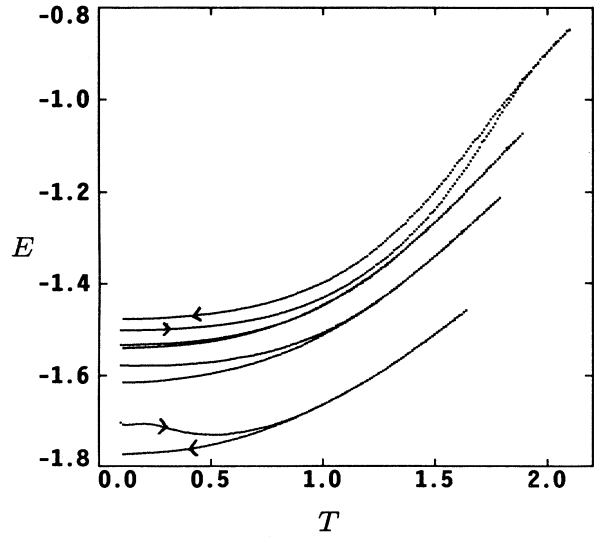

FIG. 1. Internal energy vs temperature during FH and FC, for four different magnetic fields: $B = 0.8, 1.2, 1.6, 2.2$ (from above).

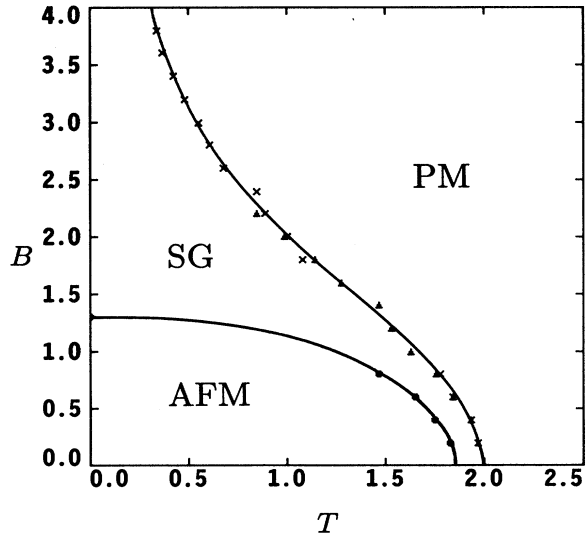

FIG. 3. Phase diagram of the DAFF for a dilution of 50% determined as explained in the text. The lines are guides to the eye only.

A very accurate determination of $B_c(T)$ for higher fields turns out to be difficult as we will argue in the following. $B_c(T)$ is expected to be nearly constant for low temperatures. In order to determine the critical line we have to cross it. This can be done by choosing a path through the phase diagram with constant temperature changing the field. A determination of the relevant critical properties like the order parameter or the energy $E(B)$ during field increasing (FI) and subsequently field decreasing (FD) has been done but the results are only in qualitative agreement with those of the corresponding FC-FH procedures. As an example Fig. 4 shows a $E(B)$ FI-FD loop for a temperature of $T = 0.4$. The rate of FI or FD was 100 MCS/point. A regime of a stable domain state between $B_{\rm eq}(T)$ and $B_c(T)$—marked by the point of intersection of the FI and FD curves—is obvious.[17] However, in these procedures we are too far away from thermal equilibrium. On the one hand the domain state is frozen even for $B \to 0$ and it shows an aging phenomena known from spin glasses: the energy can be lowered by annealing the system. At the same point in the phase diagram the energy of the domain state reached through FC is lower than the energy reached through FD. On the other hand even the long-range ordered state is frozen for higher fields and the ground state of the DAFF is nontrivial also in the low field limit where long-range order occurs (see the irreversibilities of the long-range ordered state investigated in Refs. 8 and 10).

These two facts lead to an uncertainty in the determination of $B_c(T)$ which cannot be solved just by an increase in computer time. Therefore we have excluded the results from FI-FD loops from the determination of the phase diagram and we present Fig. 4 here only for a better understanding of the change of stability in the system.

III. ANALYSIS OF THE PHASE DIAGRAM

The phase diagram shown in Fig. 3 is divided into three parts, two of which can be identified easily: the high temperature paramagnetic phase and the low temperature antiferromagnetic phase which is stable for small fields. In order to further investigate the phase diagram we have looked for the scaling behavior of $B_{\rm eq}(T)$ and $B_c(T)$. Both of them are expected to scale with $(T_N - cB^2 - T)^{\Phi_{co}/2}$ for low fields[1] where Φ_{co} is the crossover exponent from random bond to random-field behavior. Figure 5 shows a double logarithmic plot of B_c versus $T - T_N$ and $B_{\rm eq}$ versus $T - T_{\rm eq0}$ where $T_{\rm eq0} = T_{\rm eq}(B \to 0)$. The symbols correspond to those of Fig. 3. The way we have chosen to obtain the parameters is the following.

At first we neglect the correction term $-cB^2$ which is expected to be small. Fitting the three data for the lowest fields to

$$B_c = a(T_N - T)^{\Phi_{co}/2} \tag{2}$$

we get the values $\Phi_{co} = 1.41$, $T_N = 1.88$, and $a = 2.17$. Next we fitted the data of $B_{\rm eq}(T)$ in the same temperature region—i.e., using the first seven points—to

$$B_{\rm eq} = a(T_{\rm eq0} - T)^{\Phi_{co}/2} \tag{3}$$

obtaining the values $\Phi_{co} = 1.41 \pm 0.14$, $T_{\rm eq0} = 2.01$, and $a = 3.21$. As expected we get the same value of Φ_{co} as for $B_c(T)$. Apart from this the values for the crossover exponent we obtained are in very good agreement with experimental results.[8,16,18] In contradiction to experimental results $T_{\rm eq0}$ differs from T_N. This of course is also obvious in Fig. 3 and we attribute it to dynamical effects which will be discussed later.

In order to investigate the influence of the parameter c we fitted the data with a small correction term following a mean-field calculation of Cardy[19] who found $c = T_N\chi^2$, where χ is the susceptibility. Therefore we have taken a

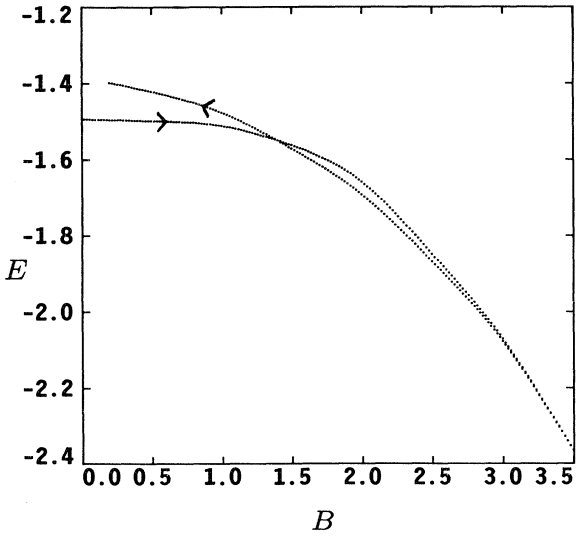

FIG. 4. Internal energy vs field during FI and FD for a temperature of $T = 0.4$.

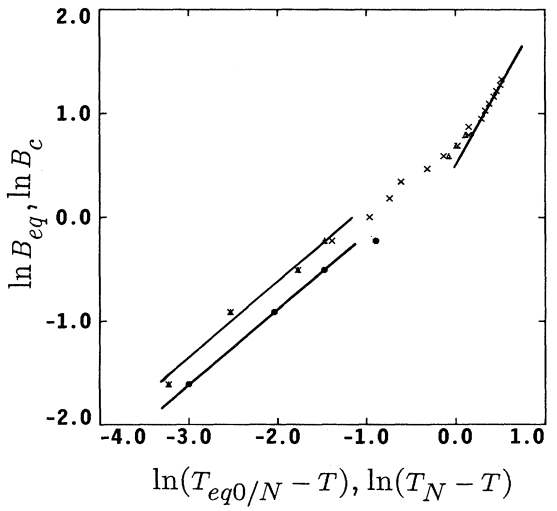

FIG. 5. Logarithmic plot of the phase diagram (see Fig. 3) as explained in the text.

value of $c = 0.01$ for the fit corresponding to $\chi = 0.07$ which is roughly in agreement with our $M(B)$ data. However, this correction did not lead to a significant change of Φ_{co}.

As is obvious from Fig. 5 and also from Fig. 3 there is a crossover to another scaling behavior for higher fields. To obtain the corresponding exponent Φ we fitted the high field data — the last seven points — to $(T_{eq0} - T)^{\Phi/2}$ using the same value for T_{eq0} as before. The value obtained, $\Phi = 3.27 \pm 0.05$ is just in between the theoretical value of $\Phi_{AT} = 3$ for a spin-glass replica symmetry breaking line[13] and the experimental value $\Phi = 3.4$ found recently in these systems.[5]

Here some comments on the dynamical effects already mentioned earlier are in order. As is well known from spin glasses the position of a dAT line depends on the cooling or heating rate which is used in experiments and simulations, respectively. In our simulations this effect could be observed also by calculating phase diagrams with $B_{eq}(T)$ obtained through runs with different heating or cooling rates. The position of the dAT line then changes as well as the value of $B_{eq}(T)$ in the crossover regime but this has practically no influence on the exponents Φ_{co} and Φ_{AT}. Note that it is even this effect that explains the difference between T_N and T_{eq0}. In the limit of very long cooling or heating rates T_{eq0} tends to T_N. The phase diagram which is shown here is the one we obtained for the slowest cooling or heating rate.

To summarize, the phase diagram we obtained is in good agreement with the works of Refs. 5 and 4. We conclude that the domain state is a stable phase between the AT line and $B_c(T)$ with the characteristics of a spin glass. In contrast to usual spin glasses the spin-glass phase here is field induced. Without an external field the system is long-range ordered and there is no frustration. In order to further investigate the nature of the domain state we now want to focus on the structure of the domains.

IV. THE STRUCTURE OF THE DOMAIN STATE

The first estimate of the influence of random fields on d-dimensional spin systems has come from Imry and Ma.[14] Their argument can easily be transferred to the DAFF: comparing the number of vacancies in a finite part of the lattice with radius R one finds a statistical surplus of vacancies in one of the antiferromagnetic sublattices. This leads to a net magnetization which couples to the homogeneous external field decreasing the energy of the system by

$$E_M \sim -BR^{d/2}. \tag{4}$$

This fact explains the existence of finite domains. On the other hand there is an increase in energy through the broken bonds in the domain wall:

$$E_W \sim R^{d-1}. \tag{5}$$

Assuming a long-range ordered 3D system, the influence of an external field cannot break long-range order because the wall energy of a growing domain crosses the volume part of the energy for increasing R. The conclusion then is that the long-range ordered state of the DAFF is the stable one and the domain state is only metastable due to energy barriers.

Of course, this is a ground-state argument in the limit of small B where the domains are assumed to be large and randomly selected so that the statistical square-root argument holds. It is further assumed that the domains are not fractal.

To further investigate these two assumptions in the limit of higher fields we have directly computed the volume V (number of spins), surface F (number of unsatisfied bonds), and radius R (root of the mean-squared distance of spins) of the domains formed. Apart from this we have calculated the wall energy (number of broken bonds) and the domain magnetization M_V in order to get a deeper insight into the stability of the domains.

The way of computing these quantities is as follows: as initial configuration we take a completely random $99 \times 99 \times 98$ system and make rapid quenches to low temperatures and high external fields, i.e., in the regime of the spin-glass phase. We then observe the development of the system by carrying out a cluster analysis with a suitable adjusted Hoshen-Kopelman-type algorithm.[20] This algorithm pieces the system into domains of connected and antiferromagnetically ordered spins. From the completely disordered state after a few MCS a domain state develops consisting of domains with sizes on all possible lengths. Surprisingly, there occur also two large percolating domains penetrating each other. Penetration is a property of the DAFF which can be observed on smaller length scales as well. The importance of penetration will be discussed later.

The two percolating clusters below $B_{eq}(T)$ could be observed also in larger systems with a size of up to $145 \times 145 \times 144$ spins—the largest system we have simulated so far.

Figure 6 shows the frozen domain state of a $99 \times 99 \times 98$ system after a relaxation time of 100 MCS for a temperature of $T = 0.4$ and a field of $B = 3.0$ (all figures shown in the following have been calculated from corresponding runs at this point in phase diagram). This system of course is not in thermal equilibrium. A real equilibrium cannot be reached even with longer thermalization due to the aging phenomenon. Very long simulations at selected values of parameters have shown that there is no qualitative change in the behavior of the system. We believe this to be the case in general so that relatively short simulation are sufficient to investigate typical domain properties. Figure 7 shows one of the smaller domains isolated by the cluster algorithm. Its size is $V = 1618$ spins.

The above procedure, rapid quench of a paramagnetic system, short thermalization, and subsequent cluster analysis is done for typically 14 lattices to get a sufficient large number (typically 100 000) of domains. The above-mentioned physical quantities are calculated and then averaged over all domains having equal volume in order to get a higher accuracy.

Figures 8 and 9 show the corresponding double logarithmic plots for V, F, and R. The large percolating

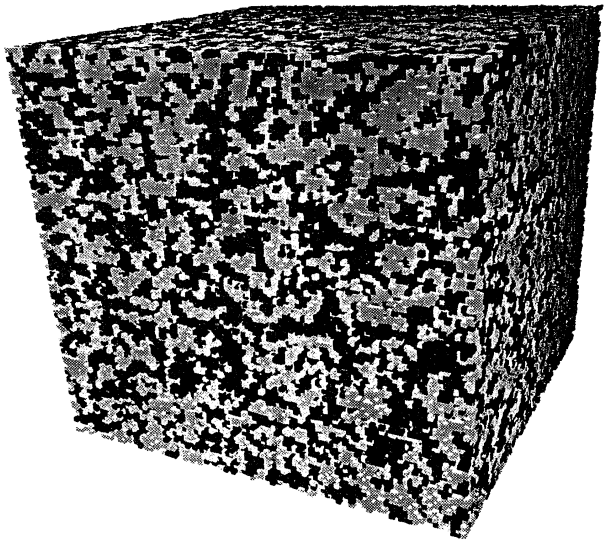

FIG. 6. Frozen domain state of a $99\times99\times98$ system. The two phases are represented in light and dark gray. Vacancies are not shown.

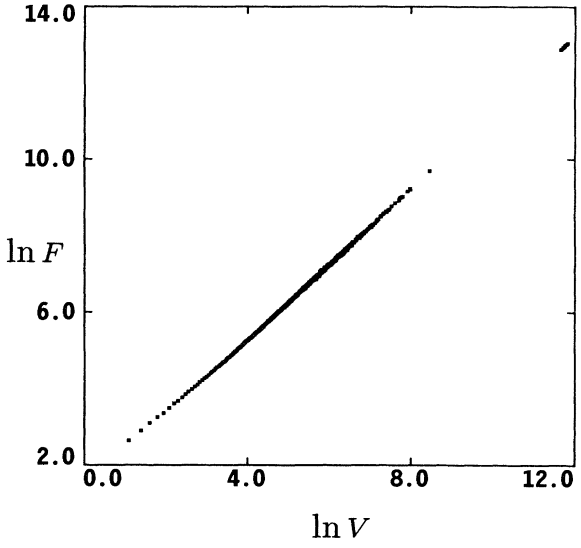

FIG. 8. $\ln F$ vs $\ln V$.

domains result in the single points for large volume in Fig. 8. A definition of R for percolating clusters in a system with periodical boundary conditions is useless, therefore the corresponding points are neglected in Fig. 9. The following scaling relations hold:

$$V \sim F \tag{6}$$

and

$$V \sim R^D \tag{7}$$

with $D = 2.0\pm0.1$. The first relation $V \sim F$ is a common feature for highly diluted objects. Because most of the surface is inside the domain the surface is proportional to the volume.[21] Much more interesting is relation (7), which means that the domains are fractal (the Euclidian dimension is $D_e = 3$). The fractal dimension $D = 2$ is known from the so-called "lattice animals" in the three-dimensional percolation problem and it has been determined exactly.[22] Our conclusion is that the magnetic domains of the DAFF show the same fractal behavior as the—in our system much smaller—clusters of the percolation problem.

It should be mentioned that the graph $R(V)$ has a small negative curvature. The value $D = 2$ is the limit for small R. In the limit of large R where our data are less accurate this value changes to $D = 2.2$. We attribute this to the above-mentioned problem of an accurate def-

FIG. 7. One typical domain of the domain state Fig. 6 with a volume of $V = 1618$ spins.

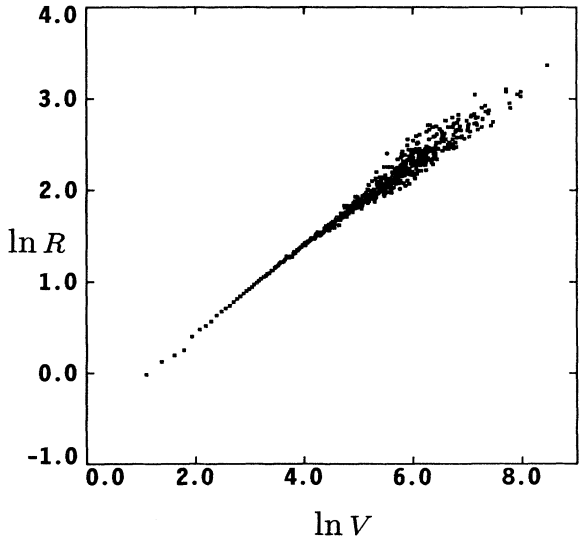

FIG. 9. $\ln R$ vs $\ln V$.

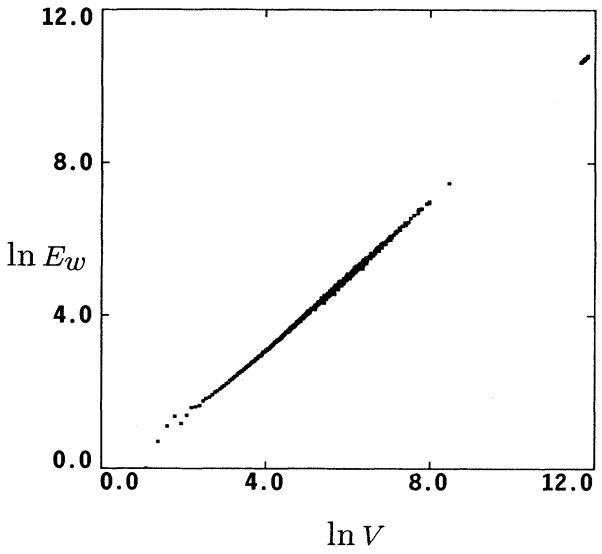

FIG. 10. $\ln E_W$ vs $\ln V$.

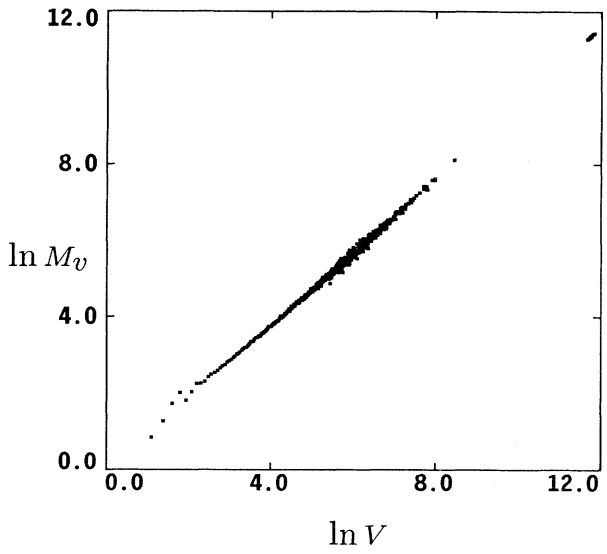

FIG. 11. $\ln M_V$ vs $\ln V$.

inition of R in finite systems: when the largest distance between spins of the same domain reaches the size of the system the mean-square deviation of the spins becomes artificially small due to the periodical boundary conditions.

Figures 10 and 11 show the scaling behavior of E_W and M_V. The following relations hold:

$$E_W = sV^{\sigma} \tag{8}$$

with $\sigma = 0.995 \pm 0.001$, $s = 0.72$, and

$$M_V = tV^{\theta} \tag{9}$$

with $\theta = 0.996 \pm 0.001$ and $t = 0.38$. From Eq. (9) we can conclude that there is a strong deviation of the scaling behavior from the usual assumptions (see also Ref. 23). This can be understood by the fact that the form of the domains is not random. Instead very complicated structures arise (see Figs. 6 and 7). Typically, domains are interpenetrating so that even large domains for which the statistical argument was thought to hold can draw advantage from random field fluctuations on small length scales. The domains then carry magnetization which is directly proportional to its volume and not to its square root.

Equation (8) is as expected $E_W \sim F$. From the equality of the two exponents θ and σ it follows that it now depends on the external field and on the prefactors s and t which contribution to the total domain energy is the most important. By doing simulations for different external fields we have found that these prefactors are slightly field dependent. However, a comparison of the prefactors shows that in the case shown here ($B = 3.0$) the energy decrease due to the domain magnetization is larger than the increase due to the domain-wall energy. This explains the stability of domains for high fields and low temperatures.

V. CONCLUSIONS

We have determined the random-bond–random-field crossover exponent within a Monte Carlo simulation. Our result $\Phi_{co} = 1.41$ is in very good agreement with experimental findings.[8,16,18]

Apart from this we have shown that there is strong evidence for the existence of a spin-glass phase in the DAFF model. The main support comes from an AT-type line which is in agreement with recent experimental and theoretical findings.[4,5] This evidence is supported by other well-known features of the DAFF like the occurrence of irreversibilities and the occurrence of thermoremanent magnetization[8,10] also typical for spin glasses. Even quantitatively the decay of the remanent magnetization agrees with that of the remanent magnetization of spin glasses: the decay follows a power law in time with the exponent proportional to the temperature.[12,24]

We have estimated the critical line $B_c(T)$. The spin-glass phase between this line and the AT line can be understood as a stable domain state. In analyzing the structure of the domains we found them to be fractal. Due to this fractality and the interpenetrating nature of the domains which are nonstatistical, the scaling of volume magnetization and wall energy important in an Imry-Ma-type argument deviates from usual assumptions and might explain the stability of the phase.

ACKNOWLEDGMENT

This work was supported by the Deutsche Forschungsgemeinschaft through Sonderforschungsbereich 166.

*Electronic address (BITNET): uli@hal9000.uni-duisburg.de.

[1] S. Fishman and A. Aharony, J. Phys. C **12**, L729 (1979).
[2] A. T. Ogielski and D. A. Huse, Phys. Rev. Lett. **56**, 1298 (1986).
[3] H. T. Diep, S. Galam, and P. Azaria, Europhys. Lett. **4**, 1067 (1987).
[4] I. Ya. Korenblit and E. F. Shender, Zh. Eksp. Teor. Fiz. **89**, 1785 (1985) [Sov. Phys. JETP **62**, 1030 (1985)]; J. R. L. de Almeida and R. Bruinsma, Phys. Rev. B **35**, 7267 (1987).
[5] F. C. Montenegro, U. A. Leitão, M. D. Coutinho-Filho, and S. M. Rezende, J. Appl. Phys. **67**, 5243 (1990); F. C. Montenegro, A. R. King, V. Jaccarino, S-J. Han, and D. P. Belanger, Phys. Rev. B **44**, 2255 (1991).
[6] G. S. Grest, C. M. Soukoulis, and K. Levin, Phys. Rev. B **33**, 7659 (1986).
[7] R. J. Birgeneau, R. A. Cowley, G. Shirane, and H. Yoshizawa, J. Stat. Phys. **34**, 817 (1984); D. P. Belanger, S. M. Rezende, A. R. King, and V. Jaccarino, J. Appl. Phys. **57**, 3294 (1985); R. A. Cowley, R. J. Birgeneu, and G. Shirane, Physica **140A**, 285 (1986).
[8] U. A. Leitão, W. Kleemann, and I. B. Ferreira, Phys. Rev. B **38**, 4765 (1988); P. Pollak, W. Kleemann, and D. P. Belanger, *ibid.* **38**, 4773 (1988).
[9] J. Villain, Phys. Rev. Lett. **52**, 1543 (1984).
[10] U. Nowak and K. D. Usadel, Phys. Rev. B **39**, 2516 (1989).
[11] T. Nattermann and I. Vilfan, Phys. Rev. Lett. **61**, 223 (1988).
[12] U. Nowak and K. D. Usadel, Phys. Rev. B **43**, 851 (1991); Physica B **165**, 211 (1990).
[13] J. R. L. de Almeida and D. J. Thouless, J. Phys. A **11**, 983 (1978).
[14] Y. Imry and S.-k. Ma, Phys. Rev. Lett. **35**, 1399 (1975).
[15] K. Binder and D. W. Heermann, *Monte Carlo Simulations in Statistical Physics* (Springer-Verlag, Berlin, 1988).
[16] W. Kleemann, A. R. King, and V. Jaccarino, Phys. Rev. B **34**, 479 (1986).
[17] Although the difference between internal E and free energy F is small for low temperatures, even a determination of $F(B)$ is possible by integrating $M(B)dB$ for constant T, yielding corresponding results.
[18] D. P. Belanger, A. R. King, V. Jaccarino, and J. L. Cardy, Phys. Rev. B **28**, 2522 (1983).
[19] J. L. Cardy, Phys. Rev. B **29**, 505 (1984).
[20] J. Hoshen and R. Kopelman, Phys. Rev. B **14**, 3428 (1976).
[21] D. Stauffer, *Introduction to Percolation Theory* (Taylor and Francis, London, 1985).
[22] G. Parisi and N. Sourlas, Phys. Rev. Lett. **46**, 871 (1981).
[23] J. A. Cambier and M. Nauenberg, Phys. Rev. B **34**, 7998 (1986).
[24] J. Bricmont and A. Kupiainen, Phys. Rev. Lett. **59**, 1829 (1987).